DOI: 10.1002/ejic.201100378

Metal Anions in Metal-Rich Compounds and Polar Intermetallics

Myung-Hwan Whangbo,*[a] Changhoon Lee,[a] and Jürgen Köhler*[b]

Dedicated to Professor John D. Corbett on the occasion of his 85th birthday

Keywords: Intermetallic phases / Zintl anions / Electronic structure / Transition metal anions / Alkali metal anions

We briefly surveyed metal-rich and intermetallic compounds containing metal anions that have been characterized by density functional calculations. Transition metal anions come with electron configurations $(n+1)s^2nd^{10}(n+1)p^0$, $(n+1)s^2nd^{10}(n+1)p^1$, and $(n+1)s^2nd^{10}(n+1)p^2$. Their *n*d orbitals act as reservoirs for holding ten electrons. Thus, these anions exhibit bonding characteristics similar to those found for their main group analogues.

1. Introduction

Compound formation among atoms with different electronegativities involves charge transfer among them. Nearly a century ago the first compound containing a transition metal anion, CsAu,[1] was characterized. It took some decades until the existence of an Au^- ion, which is stabilized by the relativistic effect,[2] was finally confirmed by measurements and calculations of the electronic structure of CsAu.[3] In 1958 Goodman claimed that in general the $nd^{10}(n+1)s^2$ configuration can be considered as a kind of closed shell like that of the $1s^2$ configuration of He and that a Pt^{2-} should also exist.[4] The stability of $(Hg_4)^{6-}$ square rings in Na_3Hg_2 has been attributed to aromaticity.[5] In this article, we give a short overview of the results of our studies on further metal-rich compounds and polar intermetallics on the basis of density functional electronic structure calculations.

[a] Department of Chemistry, North Carolina State University, Raleigh, NC 27695-8204, USA
E-mail: mike_whangbo@ncsu.edu
[b] Max-Planck-Institut für Festkörperforschung, Stuttgart, Germany
E-mail: j.koehler@fkf.mpg.de

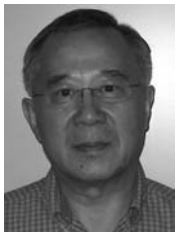

Professor M.-H. Whangbo received his bachelor's and master's degrees from Seoul National University in 1968 and 1970, respectively, and his PhD in Chemistry from Queen's University in 1974. After postdoctoral studies at Queen's and Cornell Universities, he started his academic career at North Carolina State University in 1978, where he is a Distinguished Professor of Chemistry. His research efforts have been devoted to understanding the structure–property relationships in solid state materials on the basis of electronic structure calculations and analyses.

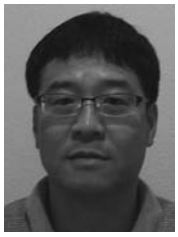

Dr. Changhoon Lee received his bachelor's and master's degrees from Wonkwang University in 1998 and 2000, respectively. After receiving his PhD in Chemistry from Wonkwang University in 2005, he joined Prof. Whangbo's research group as a postdoctoral associate and is currently a research assistant professor. He has studied the electronic structures of a wide variety of solid state materials on the basis of first principles density functional theory calculations.

Jürgen Köhler studied chemistry at the Justus-Liebig University in Gießen and wrote his dissertation with Prof. R. Hoppe in 1984. Afterwards he joined the group of Prof. A. Simon at the Max-Planck-Institute for Solid State Research, where he worked mainly on the synthesis and characterization of low-valent metal clusters containing niobium oxides and the development of a real space approach for superconductivity. After finishing his habilitation in 1993 he received the venia legendi for Inorganic Chemistry from the University of Stuttgart in 1994 and the title Professor in 2006. His main research interests are the preparation and the characterization of the structure and properties of low-valent oxides and fluorides as well as the study of polar intermetallics of the late transition elements.

2. Transition Metal Anions in Binary Compounds with Alkali Metals

In the highly ionic auride CsAu[1,3] and platinide Cs_2Pt,[6] the transition metals are in the negative oxidation states –1 and –2, respectively. In these compounds, the 6s and 5d orbitals of the Au^- and Pt^{2-} anions act as reservoirs for holding 12 electrons with an electron configuration of $6s^25d^{10}$. Late transition metals with relatively high electronegativity can also be present as anions in numerous polar intermetallics. For example, the electronic structures of the metal-rich series Pt metal, $LiPt_2$, LiPt, and Li_2Pt indicate that the 5d electron configurations of Pt in these compounds are close to $5d^{10}$ and that the Pt 5d-block bands are increasingly filled with decreasing Pt content in this series[7] (Figure 1). A similar trend is observed for the Pt 6s- and Pt 6p-block bands, which are occupied to a small percentage only.[4] In the Zintl sense, the electrons in the Li/Pt binary phases are transferred from the Li to the Pt atoms, so that the Pt atoms are best described as partially negative anions.

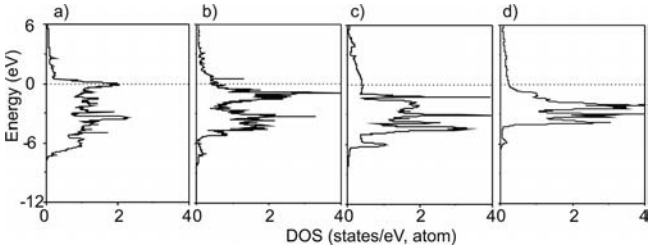

Figure 1. Partial density of states (PDOS) plots calculated for the Pt-5d-block bands in (a) Pt metal, (b) $LiPt_2$, (c) LiPt, and (d) Li_2Pt.

3. Alkali Metal Anions in Alkali Metal Clusters

Electron transfer can occur between atoms of the same element when the coordination environments of the atoms are different. For example, in the structure of α-Mn, different oxidation states are assigned to the four crystallographically different Mn atoms.[8]

A similar example of "topologically induced" charge transfer among metal atoms of the same type is also found in the metal-rich Cs compound Cs_9InO_4.[9] This complex oxoindate consists of InO_4 tetrahedra and $Cs(Cs)_{16}$ clusters as shown in Figure 2. The density of states (DOS) plots (Figure 3) obtained from density functional calculations indicate that Cs(4) located at the center of a Cs_{16} cage exists as a Cs anion. This conclusion is corroborated by the electron localization function (ELF)[10] around a $Cs(4)Cs_{16}$ polyhedron in the (002) plane containing the Cs(4), Cs(2), and Cs(3) atoms (Figure 4).

These analyses indicate that Cs_9InO_4 can be described by $(Cs^+)_8(Cs^-)[(In^{3+})(O^{2-})_4]+2e^-$, that is, it is a mixed-valence compound with Cs atoms in oxidation states +1 and –1.[11] Other examples of alkali metal anions are known from cryptand chemistry[12] and also from $Na_{16}Rb_7Sb_7$,[13] in

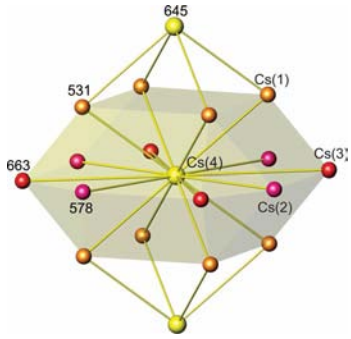

Figure 2. Perspective view of the coordination polyhedron around Cs(4) in Cs_9InO_4 together with Cs–Cs distances in pm.

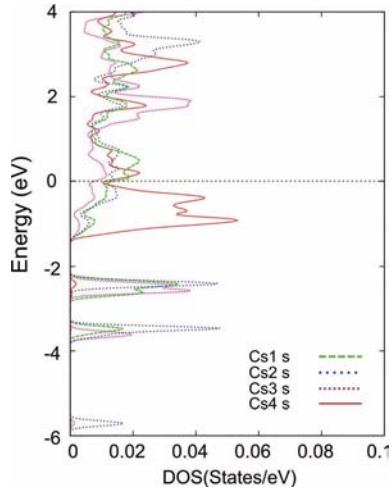

Figure 3. Partial density of states (PDOS) plots for the Cs atoms in Cs_9InO_4 (green: Cs1 s, blue: Cs2 s, black: Cs3 s, red: Cs4 s).

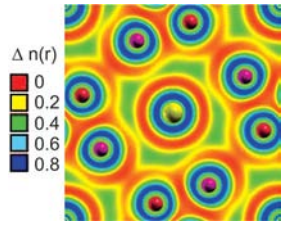

Figure 4. Distribution of ELF in the (002) plane calculated with the core states included (dark blue rings) containing the Cs(4), Cs(2), and Cs(3) atoms.

which the Rb^- anion located at the center of a $(Rb^+)_6$ octahedron can easily be replaced by an I^- or Au^- anion.[14]

Such negatively charged alkali metal ions might be less surprising for the less electropositive element Li. It would be worthwhile to search for such compounds.

4. Transition Metal Anions Encapsulated in Cationic Clusters of Group 13–15 Elements

The recently discovered compounds $PtIn_7F_{13}$,[15] $[PtIn_6](GaO_4)_2$,[16] $Pt_2In_{14}Ga_3O_8F_{15}$,[17] and $PtIn_6(GeO_4)_2O$[18] contain 18-valence-electron octahedral cations $[PtIn_6]^{10+}$

(Figure 5), in which the Pt–In bonds exhibit covalent character. The molecular orbitals of the $PtIn_6$ octahedron, calculated from extended Hückel tight binding calculations,[19] show the orbital sequence, a_{1g}, e_g, $t_{2g} < t_{1u} << e_g^* < ...$ In the a_{1g} and e_g levels, the Pt 6s and 5d orbitals, respectively, make σ bonds with the In 5s orbitals.

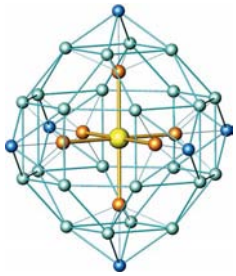

Figure 5. Perspective view of a $[PtIn_6]O_{30}$ polyhedron in $[PtIn_6](GeO_4)_2O$.

In the t_{2g} level, the Pt 5d orbitals make π bonds with the In 5p orbitals. With 18 valence electrons for $[PtIn_6]^{10+}$, the HOMO becomes the triply degenerate level, t_{1u}, in which In 5s orbitals make σ bonds with Pt 6p orbitals [Figure 6 (a)]. This HOMO level is well separated from the LUMO level, e_g^*, in which the In 5s orbitals (the major component) exhibit σ*-antibonding interactions with the Pt 5d levels [Figure 6 (b) and (c)]. As a consequence, the charge balance for $[PtIn_6]^{10+}$ is best described by $(Pt^{2-})(In^{2+})_6$, in which the Pt^{2-} and In^{2+} ions have the electron configurations $5d^{10}6s^2$ and $5s^1$, respectively. The HOMO–LUMO gap for a classical 18-electron octahedral complex such as $[PtCl_6]^{4-}$ is found between the t_{2g}^* and e_g^* levels (with major contributions from the transition metal d orbitals), whereas for $[PtIn_6]^{10+}$ it is determined by the energy difference between the t_{1u} and e_g^* levels.

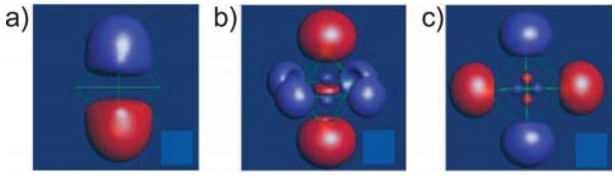

Figure 6. Boundary surface density plots calculated for (a) one of the $1t_{1u}$ and (b and c) the two degenerate $2e_g^*$ levels of a $[PtIn_6]^{10+}$ cluster.

There are other known octahedral cluster cations of main group elements encapsulating late transition metal atoms as anions, for example, $[MSn_6]^{14+}$ (M = Fe, Ru),[20] $[IrIn_6]^{9+}$,[21] and $[IrBi_6]^{n+}$ (n = 3, 4).[22] By analogy with $[PtIn_6]^{10+}$, we might assign the $d^{10}s^2$ configuration to the transition metal and the s^1 to the main group element in $[RuSn_6]^{14+}$ and $[IrIn_6]^{9+}$, so that their charge balances are described by $(Ru^{4-})(Sn^{3+})_6$ and $(Ir^{3-})(In^{2+})_6$, respectively. In the cluster cations, the nd orbitals of a transition metal act as reservoirs for holding 10 electrons, and its bonding with the surrounding main group ligands leading to the frontier energy levels takes place primarily by use of the (n+1)s and (n+1)p orbitals, so that the transition metal anions behave like a main group element.[11]

Electronic band structure calculations carried out with the linear muffin-tin orbital (LMTO) method[23] encoded in the TB-LMTO-ASA program[24] indicate that the metal atoms Pt or Ir in compounds such as $[PtIn_6](GeO_4)_2O$ (Figure 7) are best described as anions with the electron configuration $(n+1)s^2nd^{10}$. The situation is the same for all 18-electron MIn_6 octahedra with elements M of groups 8, 9, and 10, for which the oxidation states –4, –3, and –2, respectively, can therefore be assigned. Formally, this means that In has a strong power to reduce the late transition metal elements of groups 8, 9, and 10. The highest occupied bands of the compounds containing octahedral *metallo* complexes MIn_6 (M = Fe, Ni, Ru, Os, Ir, Pt) are the (n+1)-p-block bands of M and the 5s-block bands of In. These bands lie higher than the M nd-block bands, which in turn lie higher than the M (n+1)s-block bands (Figure 7). This means that the valence atomic orbital energies of the transition metal M increase in the order (n+1)s < nd < (n+1)p, in contrast to the sequence nd < (n+1)s < (n+1)p commonly found for transition metal compounds with electronegative main group elements. In general, increasing (decreasing) the number of electrons around a system increases (decreases) the extent of electron–electron repulsion and hence raises (lowers) the energies of all the orbitals of the system.[25] However, this effect does not influence all the valence atomic orbitals uniformly; a more contracted orbital is more strongly affected. For a transition metal, the nd orbital is more contracted than the (n+1)s orbital. Thus, unless the atoms surrounding a transition metal lead to strongly preferential orbital interactions with the nd, (n+1)-s, or (n+1)p orbital, the nd orbital is lowered below the (n+1)s orbital when the oxidation state of a transition metal is positive, while the nd orbital is raised above the (n+1)s orbital when the oxidation state of a transition metal is zero or negative,[26] as illustrated in Figure 8. In cases when the oxidation state of a transition metal is positive, this effect

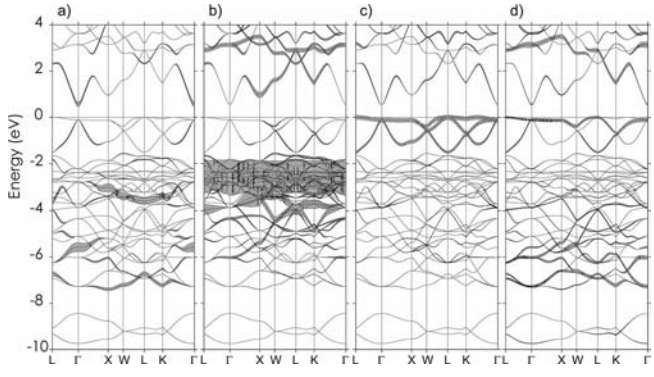

Figure 7. Dispersion relations of the energy bands calculated for $[PtIn_6](GeO_4)_2O$ with the fat band representation for (a) the 6s orbital contributions of Pt, (b) the 5d orbital contributions of Pt, (c) the 6p orbital contributions of Pt, and (d) the 5s orbital contributions of In.

also explains why the energy difference between the *n*d and (*n*+1)s levels of a transition metal atom decreases on going from the left to the right of the periodic table.

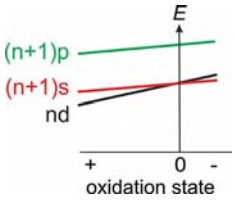

Figure 8. Schematic illustration of how the *n*d, (*n*+1)s, and (*n*+1)p orbital sequence of a transition metal element varies as a function of its oxidation state.

5. Transition Metal Dimer Anions Encapsulated in Cationic Clusters of Group 2, 3, and 13 Elements

Density functional calculations have shown that the Cr_5B_3-type compounds AE_5T_3 (*AE* = alkaline earth element; T = Au, Ag, Hg, Cd, Zn) consisting of isolated and dimeric transition metal units are best described as $[(AE^{2+})_5(T–T)^{4–}(T^{2–})]+4e^–$.[27] The isolated anions are surrounded by 10 AE^{2+} cations, which form a doubly capped square antiprism, whereas the coordination of the anionic dimers surrounded by 8 + 4AE^{2+} cations is described as two face-sharing trigonal prisms capped by four additional ligands (Figure 9).

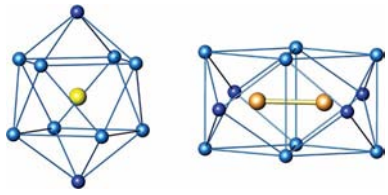

Figure 9. Coordination of isolated T(1) atoms (left) and $T(2)_2$ dimers (right) by *AE* in the Cr_5B_3-type compounds AE_5T_3, = $AE_5T(1)T(2)_2$, where *AE* = Ca or Sr, and T = Au, Ag, Hg, Cd, or Zn.

The transition metal atoms in the ternary compounds La_2Pt_2In[28] and La_2Cu_2In[29] exist also as dimeric Zintl anions $[Pt–Pt]^{6–}$ and $[Cu–Cu]^{4–}$, respectively.[30] The reason for the switching of the orbital sequence of a transition metal element from *n*d < (*n*+1)s < (*n*+1)p to (*n*+1)s < *n*d < (*n*+1)p depending on its oxidation state was clarified for the first time with these examples. $[Pt–Pt]^{6–}$, $[Au–Au]^{4–}$, $[Ag–Ag]^{4–}$, and $[Cu–Cu]^{4–}$ dimer anions are also found in the compounds Yb_3Ag_2, Ca_5Au_4, and Ca_3Hg_2,[31] in which the transition metal elements exhibit a $d^{10}s^2p^1$ configuration and behave as main group p elements forming a $p_\sigma–p_\sigma$ σ bond. The Au–Au interactions between the Au 6s orbitals within the Au–Au dimers in Dy_2Au_2In[32] have bonding and antibonding character compensating each other, which becomes evident from the COHP curves shown in Figure 10. The Au 6p-block bands show only bonding interactions between the Au 6p orbitals of each Au_2 dimer. Thus, by regarding the Au–Au bond of each Au_2 dimer as a $6p_\sigma–6p_\sigma$ single bond, the electron configuration $(6s)^2(5d)^{10}(6p)^1$ can be assigned to each Au atom, which corresponds to an $Au^{2–}$ anion. As a consequence Dy_2Au_2In can be described as $(Dy^{2+})_2[Au–Au]^{4–}In^0$ with a dimeric Zintl anion $[Au–Au]^{4–}$. A similar chemical bonding ($p_\sigma–p_\sigma$) is found for the M–M dimers in RE_2M_2In (*RE* = rare earth element, M = Pt, Cu, Au), Ca_5Au_4, Ca_3Hg_2,[31] and Ca_5M_3 (M = Cu, Au, Zn, Cd, Hg).

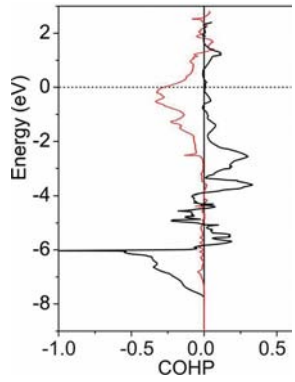

Figure 10. COHP plots calculated for the Au–Au s interactions (black) and Au–Au p interactions (red) in Dy_2Au_2In. Positive and negative values refer to antibonding and bonding interactions, respectively.

6. Transition Metal Anions Forming Tetrahedral Networks with Main Group Elements

The $s^2d^{10}p^2$ configuration of transition metal anions is found for 18-electron half-Heusler (18eHH) compounds *RE*ML (e.g., *RE* = Sc, Y; M = Ni, Pd, Au; L = As, Sn, Sb, Pb, Bi),[33] in which the M and L atoms form a diamond-like lattice (i.e., the zinc blende lattice). Most 18eHH compounds are regular semiconductors.[34,35] The electronic structure of an 18eHH compound AML (Figure 11) is described by the oxidation assignment $A^{n+}(ML)^{n–}$, where *n* is the number of valence electrons donated by A.[35a,35c] Qualitatively, the semiconducting property of most 18eHH compounds has been understood by noting that the 18-electron count around M implies a closed shell electron configuration (i.e., $d^{10} + s^2 + p^6$).

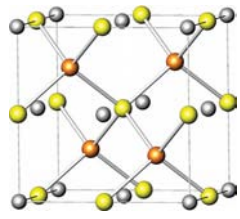

Figure 11. Perspective view of the crystal structure of a half-Heusler compound AML (A = Ca, Sc, Y, M = Au, L = Sn, Sb, Pb, Bi). The gray spheres represent the A atoms, the golden spheres the M atoms, and the yellow spheres the L atoms.

With 18 valence electrons filling the nine valence bands completely, ScAuSn is a semiconductor with a small indirect band gap[36] [Figure 12 (a)]. The partial DOS plots in Figure 12 (b) are consistent with the oxidation state +3 for Sc and hence the electron counting $[AuSn]^{3-}$. The Sn 5s and the Au 6s states are present from –8.0 to –10.0 and between –6.5 and 0.0 eV [Figure 12 (c) and (d)], with stronger Sn 5s and Au 6s contributions in the lower and higher energy regions, respectively. The Au 5d states occur primarily as sharp peaks between –6.5 and –5.0 eV, while the Au 6p states occur between –3.5 and 0.0 eV, where the Au 5d states are also present. The filled Sn 5p states occur where the filled Au 5d and the filled Au 6p states are present [Figure 12 (c) and (d)]. According to these observations, the –8.0 to –10.0 eV region represents Sn 5s/Au 6s bonding, and the –6.5 to –5.0 eV region primarily the Au 5d states with some Au 5d/Sn 5p bonding. The –3.5–0.0 eV region represents Au 5d,6p/Sn 5p bonding.

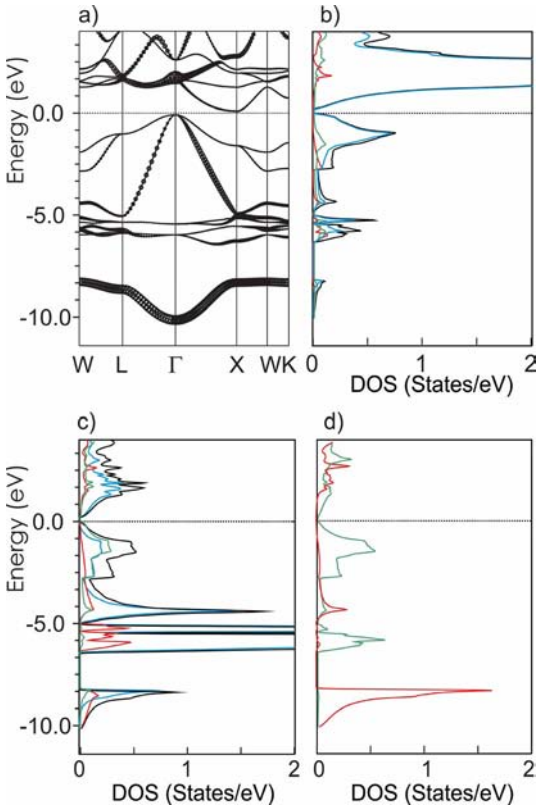

Figure 12. Calculated electronic structure of ScAuSn: (a) Dispersion relations of the bands around the Fermi level (0 eV). (b) Total (black) and partial DOS plots for Sc s (red), Sc p (green), and Sc d (blue). (c) Partial DOS plots for Au s (red), Au p (green), and Au d (blue). (d) Partial DOS plots for Sn s (red) and Sn p (green).

The Au 5d-block bands of ScAuSn are completely filled [Figure 12 (a)], hence leading to a d-electron count of $5d^{10}$, and lie well below the Fermi level so that the 10 d electrons of Au may be regarded as "pseudo-core" electrons. Then, the 18-electron rule is reduced to the octet rule for ScAuSn,[35] and each Au atom may be regarded as a "pseudo" main group element with eight valence electrons to form four polar covalent Au–Sn bonds. Thus, the covalent electron counting[37] leads to four electrons in the 6s and 6p orbitals for each Au, and hence to s- and p-electron counts of $6s^26p^2$, since the Au 6s bands are completely filled. As a result, each Au of ScAuSn has the electron configuration $(5d)^{10}(6s)^2(6p)^2$. In terms of the ionic electron counting, this configuration is equivalent to a formal Au^{3-} ion, so that the oxidation assignment is $(Sc^{3+})(Au^{3-})(Sn^0)$ for ScAuSn.

To show that the assignment of oxidation states to atoms of metallic compounds is rather useful, we consider the classical Zintl phase NaTl.[38] The crystal structure of NaTl, which has a diamond lattice made up of Tl atoms, is commonly described in terms of the Zintl electron counting Na^+Tl^-, because the Tl^- anions with four valence electrons are expected to form a diamond lattice as do carbon atoms. However, unlike diamond, NaTl is a metal simply because its p-block bands are not completely filled.[36] This shows also that a description of a metallic compound in terms a Zintl-like phase is reasonable and can be useful. For numerous main group element compounds, for example Ca_5Ge_3, Zintl-like behavior in connection with metallic conductivity has already been accepted.

7. Valence Orbitals of Cations Stabilizing Metal Anions

So far, our discussion has been focused on the metal anions. It should be noted that these anions are surrounded by cations of group 1–3 elements. In general, when a neutral atom becomes a cation, its orbitals are contracted and lowered in energy. As a consequence, alkali cations A^+ possess low-lying *n*p orbitals effective in forming covalent bonds with the surrounding anions, and these *n*p orbitals provide a directional character for the covalent bonding that the *n*s orbitals cannot. In a similar manner, the alkaline earth AE^{2+} and rare earth RE^{3+} cations possess low-lying (*n*–1)d orbitals effective in forming covalent bonds with the surrounding anions, and these (*n*–1)d orbitals provide a more directional character for the covalent bonding than the *n*s and *n*p orbitals can. The covalent bonding between anions and cations is not strong, because the orbital overlap between them involves their diffuse orbitals. Nevertheless, these weak interactions are important for stability. For example, in the bonding of alkali cations A^+ with the surrounding anions, the *n*p orbitals of these cations contribute more than their *n*s orbitals, as found for Cs_2CuCl_4[39] as well as for $LiPt_2$, LiPt, and Li_2Pt.[40] In the bonding of alkaline earth AE^{2+} and rare earth RE^{3+} cations with the surrounding anions, the (*n*–1)d orbitals of these cations contribute more than their *n*s and *n*p orbitals, as found for the intermetallic compounds ScAuSn, $LaPt_2In$, Ca_3Hg_2, and Yb_3Ag_2, as well as for normal Zintl compounds such as Ca_5Ge_3[41] and CaC_2.[42]

8. Concluding Remarks

Our electronic structure studies on the basis of density functional electronic structure calculations for polar inter-

metallic compounds with late transition elements have shown that the transition metals exist as anions with the valence electron configuration $(n+1)s^2nd^{10}(n+1)p^1$ or $(n+1)s^2nd^{10}(n+1)p^2$, and the frontier orbitals of these compounds are described by the $(n+1)$p orbitals of the transition metal rather than by the nd orbitals. The essential qualitative picture emerging from these electronic structure studies is as follows: For a large number of intermetallic compounds containing late 3d–5d transition metal atoms and electropositive elements, the presence of transition metal anions is manifested by the fact that the frontier orbitals of these compounds are not described by the transition metal nd orbitals but by the transition metal $(n+1)$p orbitals. Figure 13 compares the electron configurations for the probable anions of late main group and late transition metal elements with comparable bonding capability. In general, many more of such polar intermetallic compounds can be classified in terms of an extended Zintl concept including the late transition elements. The number of p electrons on a transition metal determines the structural units it forms. For example, a discrete anion is found for the pseudo-closed-shell configuration $(n+1)s^2nd^{10}(n+1)p^0$ corresponding to an ns^2np^6 configuration of a main group element (Figure 13). A transition metal anion T with $(n+1)s^2nd^{10}(n+1)p^1$ configuration forms T–T dumbbells, an analogue of main group dumbbells associated with the ns^2np^5 configuration. Transition metal anions T with $(n+1)s^2nd^1(n+1)p^2$ configuration lead to a tetrahedral coordination, as found for the diamond-like framework of semiconducting 18 electron half-Heusler compounds. It is an interesting question whether such transition metal anions can form chains of transition metal atoms as do the main group elements S, Se, or Te with ns^2np^4 configuration. In numerous compounds containing transition metal atoms with configuration close to $(n+1)s^1nd^{10}(n+1)p^0$, they form chains, as found for $LiPt_2$[7] or BaPt.[43]

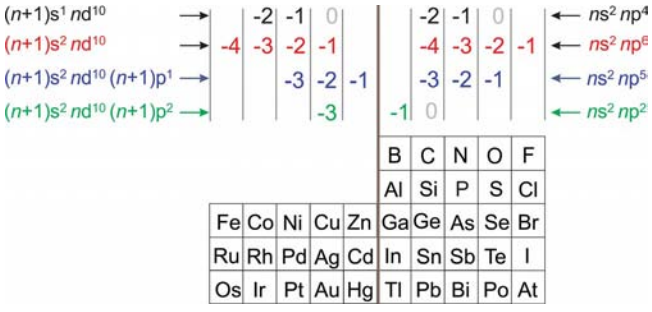

Figure 13. Oxidation states and valence electron configurations of the anions associated with late transition metal and main group elements. The colors black, red, blue, and green indicate the tendency to form chains, discrete anions, dumbbells, and diamond-like frameworks, respectively.

Acknowledgments

M.-H. W. acknowledges the financial support from the Office of Basic Energy Sciences, Division of Materials Sciences, U. S. Department of Energy, under Grant DE-FG02-86ER45259 and thanks the National Energy Research Scientific Computing (NERSC) and the High Performance Computing (HPC) Centers for their computer resources.

[1] A. H. Sommer, *Nature* **1943**, *152*, 215.
[2] a) P. Pyykkö, *Chem. Rev.* **1988**, *88*, 563; b) P. Pyykkö, *Angew. Chem. Int. Ed.* **2002**, *41*, 3573–3578.
[3] a) V. E. Wood, J. R. Reitz, *J. Phys. Chem. Solids* **1962**, *23*, 229; b) T. L. Liu, *Phys. Rev.* **1975**, *12*, 3008; c) A. Hasegawa, M. Watabe, *J. Phys. F* **1977**, *7*, 75; d) J. Knecht, R. Fischer, H. Overhof, F. Hensel, *J. Chem. Soc., Chem. Commun.* **1978**, 905; e) G. K. Wertheim, R. L. Cohen, G. Crecelius, K. W. West, J. H. Wemick, *Phys. Rev. B* **1979**, *20*, 860.
[4] C. H. L. Goodman, *J. Phys. Chem. Solids* **1958**, *6*, 305.
[5] A. E. Kuznetsov, J. D. Corbett, L.-S. Wang, A. I. Boldyrev, *Angew. Chem.* **2001**, *113*, 3473; *Angew. Chem. Int. Ed.* **2001**, *40*, 3369.
[6] A. S. Karpov, J. Nuss, U. Wedig, M. Jansen, *Angew. Chem.* **2003**, *115*, 4966; *Angew. Chem. Int. Ed.* **2003**, *42*, 4818.
[7] C. Lee, M.-H. Whangbo, J. Köhler, *J. Comput. Chem.* **2008**, *29*, 2154.
[8] a) J. A. Oberteufer, J. A. Marcus, L. H. Schwartz, G. P. Felcher, *Phys. Lett. A* **1968**, *28*, 267; b) V. Sliwko, P. Mohn, K. Schwarz, *J. Phys. Condens. Matter* **1994**, *6*, 6557.
[9] C. Hoch, J. Bender, A. Simon, *Angew. Chem.* **2009**, *121*, 2451; *Angew. Chem. Int. Ed.* **2009**, *48*, 2415.
[10] a) A. D. Becke, K. E. Edgecombe, *J. Chem. Phys.* **1990**, *92*, 5397; b) A. Savin, O. Jepsen, J. Flad, O. K. Andersen, H. Preuss, H. G. von Schnering, *Angew. Chem.* **1992**, *104*, 186; *Angew. Chem. Int. Ed. Engl.* **1992**, *31*, 187; c) B. Silvi, A. Savin, *Nature* **1994**, *371*, 683.
[11] C. Hoch, A. Simon, C. Lee, M.-H. Whangbo, J. Köhler, *Z. Kristallogr. Cryst. Mater.* **2011**, *226*, 553.
[12] J. L. Dye, *Angew. Chem.* **1979**, *91*, 613; *Angew. Chem. Int. Ed. Engl.* **1979**, *18*, 587.
[13] H.-G. v. Schnering, R. H. Cardoso Gil, W. Hönle, A. Burkhardt, G. Krier, O. K. Andersen, *Angew. Chem. Int. Ed. Engl.* **1995**, *34*, 1.
[14] H.-G. v. Schnering, R. H. Cardoso Gil, W. Hönle, N. Caroca Canales, K. Peters, *Z. Anorg. Allg. Chem.* **1996**, *622*, 112.
[15] J. Köhler, J.-H. Chang, *Angew. Chem.* **2000**, *112*, 2077; *Angew. Chem. Int. Ed.* **2000**, *39*, 1998.
[16] H. A. Friedrich, J. Köhler, *Z. Anorg. Allg. Chem.* **2001**, *627*, 144.
[17] J. Köhler, J.-H. Chang, M.-H. Whangbo, *J. Am. Chem. Soc.* **2005**, *127*, 2277.
[18] J. Köhler, H. A. Friedrich, M.-H. Whangbo, A. Villesuzanne, *J. Am. Chem. Soc.* **2005**, *127*, 12990.
[19] Calculations were carried out by employing the CAESAR2 program package: D. Dai, J. Ren, W. Liang, M.-H. Whangbo, http://chvamw.chem.ncsu.edu/, **2002**.
[20] a) T. Söhnel, P. Böttcher, W. Reichelt, F. E. Wagner, *Z. Anorg. Allg. Chem.* **1998**, *624*, 708; b) T. Söhnel, W. Reichelt, F. E. Wagner, *Z. Anorg. Allg. Chem.* **2000**, *626*, 223; c) W. Reichelt, T. Söhnel, O. Rademacher, H. Oppermann, H. Mattausch, A. Simon, J. Köhler, *Angew. Chem.* **1995**, *107*, 2307; *Angew. Chem. Int. Ed. Engl.* **1995**, *34*, 2113.
[21] J. Köhler, H. A. Friedrich, M.-H. Whangbo, *Z. Anorg. Allg. Chem.* **2007**, *633*, 1464.
[22] M. Ruck, *Z. Anorg. Allg. Chem.* **1998**, *624*, 521.
[23] a) O. K. Andersen, *Phys. Rev. B* **1975**, *12*, 3060; b) O. K. Andersen, O. Jepsen, *Phys. Rev. Lett.* **1984**, *53*, 2571; c) O. K. Andersen, C. Arcangeli, R. W. Tank, T. Saha-Dasgupta, G. Krier, O. Jepsen, I. Dasgupta, *Mater. Res. Soc. Symp. Proc.* **1998**, *491*, 3.
[24] G. Krier, O. Jepsen, A. Burkhardt, O. K. Andersen, *The TB-LMTO-ASA Program*, version 4.7.
[25] T. A. Albright, J. K. Burdett, M.-H. Whangbo, *Orbital Interactions in Chemistry*, Wiley, New York, **1985**.

[26] M.-H. Whangbo, C. Lee, J. Köhler, *Angew. Chem.* **2006**, *118*, 7627; *Angew. Chem. Int. Ed.* **2006**, *45*, 7465.
[27] C. Lee, M.-H. Whangbo, J. Köhler, *Z. Anorg. Allg. Chem.* **2010**, *636*, 36.
[28] D. Kaczorowski, P. Rogl, K. Hiebl, *Phys. Rev. B: Condens. Matter* **1996**, *54*, 9891.
[29] O. V. Dmytrakh, Y. M. Kalychak, *Russ. Metall. (Engl. Transl.)* **1990**, *6*, 199.
[30] M.-H. Whangbo, C. Lee, J. Köhler, *Angew. Chem.* **2006**, *118*, 7627; *Angew. Chem. Int. Ed.* **2006**, *45*, 7465.
[31] J. Köhler, M.-H. Whangbo, *Chem. Mater.* **2008**, *20*, 2751.
[32] J. Köhler, M.-H. Whangbo, *Solid State Sci.* **2008**, *10*, 449.
[33] C. P. Sebastian, H. Eckert, S. Rayaprol, R.-D. Hoffmann, R. Pöttgen, *Solid State Sci.* **2006**, *8*, 560, and references therein.
[34] C. Lee, M.-H. Whangbo, J. Köhler, *Z. Anorg. Allg. Chem.* **2007**, *633*, 2631.
[35] a) D. Jung, H.-J. Koo, M.-H. Whangbo, *THEOCHEM* **2000**, *527*, 113; b) I. Galanakis, P. H. Dederichs, N. Papanikolaou, *Phys. Rev. B* **2002**, *66*, 134428; c) H. C. Kandpal, C. Felser, R. Seshadri, *J. Phys. D: Appl. Phys.* **2006**, *39*, 776.
[36] J. Köhler, S. Deng, C. Lee, M.-H. Whangbo, *Inorg. Chem.* **2007**, *46*, 1957.
[37] For further discussions of the covalent, ionic, and modified electron counting schemes see: a) K.-S. Lee, H.-J. Koo, D. Dai, J. Ren, M.-H. Whangbo, *Inorg. Chem.* **1999**, *38*, 340; b) K.-S. Lee, H.-J. Koo, D. Dai, J. Ren, M.-H. Whangbo, *J. Solid State Chem.* **1999**, *147*, 11.
[38] E. Zintl, G. Woltersdorf, *Z. Elektrochem.* **1935**, *41*, 876.
[39] C. Lee, J. Kang, K. H. Lee, M.-H. Whangbo, *Inorg. Chem.* **2009**, *48*, 4185.
[40] C. Lee, M.-H. Whangbo, J. Köhler, *J. Comput. Chem.* **2008**, *29*, 2154.
[41] A.-V. Mudring, J. D. Corbett, *J. Am. Chem. Soc.* **2004**, *126*, 5277.
[42] S. Deng, A. Simon, J. Köhler, *Angew. Chem.* **2008**, *120*, 6805; *Angew. Chem. Int. Ed.* **2008**, *47*, 6703.
[43] A. Karpov, J. Nuss, U. Wedig, M. Jansen, *J. Am. Chem. Soc.* **2004**, *126*, 14123.

Received: April 7, 2011
Published Online: July 19, 2011

